FREQUENCY-DOMAIN EXTENDED MODELS FOR EQUALIZATION OF DOUBLY-SELECTIVE CHANNELS

Luca Rugini and Paolo Banelli

University of Perugia, D.I.E.I., 06125 Perugia, Italy

ABSTRACT

We consider frequency-domain equalization of single-carrier systems in doubly-selective channels. In this framework, we investigate the role of channel extension in the time domain on the performance of extended frequency-domain equalization. Specifically, we propose a new low-complexity channel extension technique, whose comparison with other techniques is performed by evaluating the approximation error of the channel matrix and the BER of banded linear MMSE equalizers.

Index Terms— Doubly-selective channels, frequency-domain equalization, channel extension

1. INTRODUCTION

Block transmissions have been widely investigated in the last decade [1]. Among them, the great success of orthogonal frequency-division multiplexing (OFDM) is mostly due to its capability to convert frequency-selective channels into a set of parallel frequency-flat channels, which can be easily equalized by single-tap equalizers in the frequency domain [1]. Block single-carrier (SC) systems, equipped with either zero padding or cyclic-prefix time guards [1] [2], are the natural OFDM counterparts that keep the easy frequency-domain equalization property while reducing the peak-to-average power ratio problem.

Several papers [3,4,5,6] have proved that, in OFDM systems, frequency-domain equalization with moderate complexity increase is still possible also in time-varying channels. Indeed, although the overall frequency-domain channel matrix is no longer diagonal, due to the Doppler effect that introduces intercarrier interference, it is possible to take equalization complexity under control by exploiting the approximately banded structure of the frequency-domain channel matrix, which is caused by the finite support of the Doppler spread.

Basically, the low-complexity equalizers [3,4,5,6] assume a perfect banded structure in the frequency-domain channel matrix, neglecting in their expressions the (small) channel modeling error. Recently, similar approaches for frequency-domain equalization of doubly-selective channels have been investigated also for SC systems, as in [7,8,9], where it was shown that such block equalization philosophy can be devised also for classical SC systems, which are not equipped with time guards between data blocks and are consequently prone to interblock interference (IBI).

In order to control the IBI, [7] and [8] proposed to opportunely design a receiver window in the time domain, while [9] proposed to cancel the IBI from the previous received blocks by a data-driven approach. Although a comparison between the two philosophies would deserve to be investigated, in this paper we will consider SC systems where the IBI is not present, either because deterministically eliminated by appropriate zero-padding time guards, or by assuming a perfect IBI cancellation as in the approach suggested in [9]. Conversely, aim of this paper is to focus on the extended channel equalization philosophy that has been recently introduced in [8] and [9], in order to increase the resolution capability of the equalizer in the Doppler-frequency domain. Specifically, we highlight the differences between the approaches proposed in [8] and [9], and also propose a new extended channel model which is characterized by a good performance-complexity trade-off with respect to the other two solutions. To this end, we will investigate by simulations the impact of the different channel extensions on the banded structure of the extended channel matrix in the frequency domain. Finally, we investigate the impact of the band approximation error on the BER performance of SC systems equipped with linear minimum mean-squared error (LMMSE) equalizers that assume a perfect banded structure of the frequency-domain extended channel matrix.

2. SYSTEM MODEL

We assume that the physical-layer data, transmitted in the time domain, are parsed in blocks that contain D symbols each. We also assume that a pilot block of length P is inserted between two consecutive data blocks. These pilot blocks can be used to estimate the impulse response of the channel. We denote with $\mathbf{d}$ the D-dimensional vector that represents a generic data block, with covariance expressed by $\mathbf{C}_{\mathbf{dd}} = \sigma_d^2 \mathbf{I}_D$, and with $\mathbf{p}$ the P-dimensional vector that contains the training symbols of a generic pilot block.

The signal stream is transmitted through a doubly-selective channel, i.e., a multipath channel with significant time-variation. The discrete-time equivalent impulse response of the channel can be expressed by

$$h[n,l] = h_c(nT_S, lT_S), \tag{1}$$

where T_S is the sampling period, n is the time index, and l is the lag index. We assume that both the impulse responses of the transmit and the receive pulse-shaping filters are included into the continuous-time channel impulse response $h_c(t,\tau)$. We also assume that the maximum channel delay spread L is smaller than the pilot duration P, which im-

plies $h[n,l] \neq 0$ only when $0 \leq l < L \leq P$.

By assuming both time and frequency synchronization at the receiver, the input-output relation in the time domain can be expressed by

$$\mathbf{y}_\mathrm{t} = \mathbf{H}_\mathrm{t}\,\mathbf{x}_\mathrm{t} + \mathbf{i}_\mathrm{t} + \mathbf{n}_\mathrm{t}, \tag{2}$$

where $\mathbf{y}_\mathrm{t}$ is the received block of size $N = D + P$, $\mathbf{H}_\mathrm{t}$ is a banded lower triangular $N \times N$ matrix that represents the doubly-selective channel, with element (n,l) defined by $[\mathbf{H}_\mathrm{t}]_{n,l} = h[n, n-l]$ for $0 \leq n,l \leq N-1$, $\mathbf{x}_\mathrm{t} = [\mathbf{d}^T \ \mathbf{p}^T]^T$ is the current transmitted block, $\mathbf{i}_\mathrm{t}$ contains the IBI, due to the multipath effect of the previous pilot block, and $\mathbf{n}_\mathrm{t}$ is the zero-mean additive white Gaussian noise (AWGN) vector, with covariance $\mathbf{C}_{\mathbf{n}_\mathrm{t}\mathbf{n}_\mathrm{t}} = \sigma_n^2 \mathbf{I}_N$. We assume that the channel impulse response $h[n,l]$ is perfectly known to the receiver. Hence, the IBI term $\mathbf{i}_\mathrm{t}$ is assumed known and perfectly compensated for. Noteworthy, the IBI is absent also when zero-padded pilot blocks with $P \geq 2L+1$ are used, as in the training scheme suggested in [10].

3. EXTENDED FREQUENCY-DOMAIN EQUALIZATION

In order to compensate for the channel matrix $\mathbf{H}_\mathrm{t}$ in (2), a common way is to perform linear equalization, such as LMMSE, in the time domain [11]. However, this approach requires to solve a banded triangular linear system whose complexity is $O(NL^2)$, which is cumbersome for channels with long delay spreads.

A second option is to design the LMMSE equalizer in the frequency domain. Let us denote with $\mathbf{F}_N$ the $N \times N$ unitary discrete DFT matrix, and define $\mathbf{y}_\mathrm{f} = \mathbf{F}_N \mathbf{y}_\mathrm{t}$, $\mathbf{x}_\mathrm{f} = \mathbf{F}_N \mathbf{x}_\mathrm{t}$, $\mathbf{n}_\mathrm{f} = \mathbf{F}_N \mathbf{n}_\mathrm{t}$, and

$$\mathbf{H}_\mathrm{f} = \mathbf{F}_N \mathbf{H}_\mathrm{t} \mathbf{F}_N^H. \tag{3}$$

From these definitions, by using the zero-IBI assumption, it is easy to show that (2) becomes

$$\mathbf{y}_\mathrm{f} = \mathbf{H}_\mathrm{f}\,\mathbf{x}_\mathrm{f} + \mathbf{n}_\mathrm{f}. \tag{4}$$

The LMMSE equalization can be expressed by [11]

$$\hat{\mathbf{x}}_\mathrm{f} = \mathbf{C}_{\mathbf{x}_\mathrm{f}\mathbf{x}_\mathrm{f}} \mathbf{H}_\mathrm{f}^H (\mathbf{H}_\mathrm{f} \mathbf{C}_{\mathbf{x}_\mathrm{f}\mathbf{x}_\mathrm{f}} \mathbf{H}_\mathrm{f}^H + \mathbf{C}_{\mathbf{n}_\mathrm{f}\mathbf{n}_\mathrm{f}})^{-1} \mathbf{y}_\mathrm{f}, \tag{5}$$

where the time-domain data can be recovered using $\hat{\mathbf{x}}_\mathrm{t} = \mathbf{F}_N^H \hat{\mathbf{x}}_\mathrm{f}$, the matrix $\mathbf{C}_{\mathbf{x}_\mathrm{t}\mathbf{x}_\mathrm{t}}$ represents the data covariance, $\mathbf{C}_{\mathbf{x}_\mathrm{f}\mathbf{x}_\mathrm{f}} = \mathbf{F}_N \mathbf{C}_{\mathbf{x}_\mathrm{t}\mathbf{x}_\mathrm{t}} \mathbf{F}_N^H$ and $\mathbf{C}_{\mathbf{n}_\mathrm{f}\mathbf{n}_\mathrm{f}} = \mathbf{F}_N \mathbf{C}_{\mathbf{n}_\mathrm{t}\mathbf{n}_\mathrm{t}} \mathbf{F}_N^H$. The frequency-domain equalization approach for single-carrier systems, originally suggested by [2], is characterized by a very low complexity when the channel is time invariant. Indeed, in this special case, the linear system to be solved is diagonal, like in OFDM transmissions. (The circularity of the time-domain channel matrix can be imposed in many ways, e.g., by using periodic pilots.)

For time-varying channels, although the linear system is no longer diagonal, low complexity equalization is still possible when the LMMSE equalizer in (5) is approximated by employing a structured approximated channel matrix instead of the exact $\mathbf{H}_\mathrm{f}$. For instance, the frequency-domain channel matrix can be approximated by its banded version [3]

$$\mathbf{H}_\mathrm{f}^{(Q)} = \mathbf{H}_\mathrm{f} \circ \mathbf{T}_N^{(Q)}, \tag{6}$$

where $\mathbf{T}_N^{(Q)}$ is a circulant matrix with first row equal to $[\mathbf{1}_{1\times Q+1} \ \mathbf{0}_{1\times N-(2Q+1)} \ \mathbf{1}_{1\times Q}]$, the symbol $\circ$ represents the Hadamard (i.e., element-wise) product between two matrices, and Q is a design parameter. By this approximation, the equalization in (5) becomes

$$\hat{\mathbf{x}}_\mathrm{f}^{(Q)} = \mathbf{C}_{\mathbf{x}_\mathrm{f}\mathbf{x}_\mathrm{f}} \mathbf{H}_\mathrm{f}^{(Q)H} (\mathbf{H}_\mathrm{f}^{(Q)} \mathbf{C}_{\mathbf{x}_\mathrm{f}\mathbf{x}_\mathrm{f}} \mathbf{H}_\mathrm{f}^{(Q)H} + \mathbf{C}_{\mathbf{n}_\mathrm{f}\mathbf{n}_\mathrm{f}})^{-1} \mathbf{y}_\mathrm{f}, \tag{7}$$

and obviously $\hat{\mathbf{x}}_\mathrm{t}^{(Q)} = \mathbf{F}_N^H \hat{\mathbf{x}}_\mathrm{f}^{(Q)}$. The reason behind the banded approximation of (6) lies in the limited Doppler support of the channel time variation, which renders negligible the elements of $\mathbf{H}_\mathrm{f}$ far away from the main diagonal. As a consequence of the banded approximation, the complexity of the frequency-domain banded equalizer is $O(NQ^2)$, which is significantly smaller than the time-domain approach when $Q \ll L$.

To enhance the performance of banded equalizers, recently, a third type of equalization has been proposed in [8] and [9]. The common idea of both methods is to increase the number of degrees of freedom of the equalizer by performing the equalization step in a frequency-domain with higher resolution. This is accomplished by using a DFT of dimension $U > N$ on the received vector. Let us define

$$\mathbf{y}_\mathrm{et} = [\mathbf{y}_\mathrm{t}^T \ \mathbf{0}_{1\times U-N}]^T, \tag{8}$$

which represents the zero-padded received vector. To highlight the higher dimension of the time-domain vectors, this domain will be referred to as the *extended time domain*. We can rewrite the input-output relation as

$$\mathbf{y}_\mathrm{et} = \mathbf{H}_\mathrm{et}\,\mathbf{x}_\mathrm{et} + \mathbf{n}_\mathrm{et}, \tag{9}$$

with $\mathbf{x}_\mathrm{et} = [\mathbf{x}_\mathrm{t}^T \ \mathbf{x}_\mathrm{L}^T]^T$, $\mathbf{n}_\mathrm{et} = [\mathbf{n}_\mathrm{t}^T \ \mathbf{n}_\mathrm{L}^T]^T$, and

$$\mathbf{H}_\mathrm{et} = \begin{bmatrix} \mathbf{H}_\mathrm{UL} & \mathbf{H}_\mathrm{UR} \\ \mathbf{H}_\mathrm{LL} & \mathbf{H}_\mathrm{LR} \end{bmatrix}, \tag{10}$$

where $\mathbf{H}_\mathrm{UL} = \mathbf{H}_\mathrm{t}$, and $\mathbf{x}_\mathrm{L}$, $\mathbf{n}_\mathrm{L}$, $\mathbf{H}_\mathrm{UR}$, $\mathbf{H}_\mathrm{LL}$, and $\mathbf{H}_\mathrm{LR}$ are design parameters that should satisfy the following constraints

$$\mathbf{H}_\mathrm{UR}\,\mathbf{x}_\mathrm{L} = \mathbf{0}_{N\times 1}, \tag{11}$$

$$\mathbf{H}_\mathrm{LL}\,\mathbf{x}_\mathrm{t} + \mathbf{H}_\mathrm{LR}\,\mathbf{x}_\mathrm{L} + \mathbf{n}_\mathrm{L} = \mathbf{0}_{U-N\times 1}. \tag{12}$$

By performing a DFT of dimension U, we obtain the input-output relation in the *extended frequency domain*. This relation, which is formally similar to (4), is expressed by

$$\mathbf{y}_\mathrm{ef} = \mathbf{H}_\mathrm{ef}\,\mathbf{x}_\mathrm{ef} + \mathbf{n}_\mathrm{ef}, \tag{13}$$

where $\mathbf{y}_\mathrm{ef} = \mathbf{F}_U \mathbf{y}_\mathrm{et}$, $\mathbf{x}_\mathrm{ef} = \mathbf{F}_U \mathbf{x}_\mathrm{et}$, $\mathbf{n}_\mathrm{ef} = \mathbf{F}_U \mathbf{n}_\mathrm{et}$, and

$$\mathbf{H}_\mathrm{ef} = \mathbf{F}_U \mathbf{H}_\mathrm{et} \mathbf{F}_U^H. \tag{14}$$

The banded LMMSE equalizer of (7), in the extended frequency domain, can be expressed as

$$\hat{\mathbf{x}}_\mathrm{ef}^{(Q)} = \mathbf{C}_{\mathbf{x}_\mathrm{ef}\mathbf{x}_\mathrm{ef}} \mathbf{H}_\mathrm{ef}^{(Q)H} (\mathbf{H}_\mathrm{ef}^{(Q)} \mathbf{C}_{\mathbf{x}_\mathrm{ef}\mathbf{x}_\mathrm{ef}} \mathbf{H}_\mathrm{ef}^{(Q)H} + \mathbf{C}_{\mathbf{n}_\mathrm{ef}\mathbf{n}_\mathrm{ef}})^{-1} \mathbf{y}_\mathrm{ef}, \tag{15}$$

$$\mathbf{H}_\mathrm{ef}^{(Q)} = \mathbf{H}_\mathrm{ef} \circ \mathbf{T}_U^{(Q)}, \tag{16}$$

$$\hat{\mathbf{x}}_\mathrm{et}^{(Q)} = \mathbf{F}_U^H \hat{\mathbf{x}}_\mathrm{ef}^{(Q)}. \tag{17}$$

The main feature of the extended-domain equalizers is the extra degrees of freedom that can be exploited to achieve a given goal. For instance, one goal could be to increase the performance, e.g., by reducing the band approximation error. In this view, receiver windowing could be coupled with

the channel extension method [8]. Another goal could be to constrain the computational complexity increase. Indeed, the computational complexity is $O(UQ^2)$, and hence is U/N times higher than in the conventional frequency domain.

In the following, we review different already-known choices for the channel matrix extension in (10), highlighting features and drawbacks of each option. This will guide us in proposing a new design choice. We will not consider receiver windowing, whose design is different depending on the type of domain (extended [8] and conventional [7]) and on the type of channel extension. The detailed performance comparison of known and new choices for the channel extension will be carried out in Section 4, with the help of some simulation results.

3.1. True Channel (TC) Extension

The natural way to extend the time-domain channel matrix is to use the extension of the true channel (TC), either towards the "future" or towards the "past". Specifically, in the "future" case, the extended time-domain channel matrix is expressed by

$$[\mathbf{H}_{\mathrm{t}}]_{n,l} = h[n, n-l], \quad 0 \le n, l \le U-1. \tag{18}$$

If we look at the continuous-time channel paths, the TC extension guarantees the continuity of the time variation of the channel path. In the "past" case, the channel extension is analogous to the "future" case. The only difference is that the zero padding of (8) must be replaced by trailing zeros. In case of estimated channels, a "past" extension could be more practical, since the "future" extension requires a larger equalization delay.

3.2. Zero-Padding (ZP) Channel Extension

An alternative choice is the zero-padding (ZP) channel extension [9], characterized by

$$\mathbf{H}_{\mathrm{UR}} = \mathbf{0}_{N \times U-N}, \quad \mathbf{H}_{\mathrm{LL}} = \mathbf{0}_{U-N \times N}, \quad \mathbf{H}_{\mathrm{LR}} = \mathbf{0}_{U-N \times U-N}, \tag{19}$$

and by $\mathbf{n}_{\mathrm{L}} = \mathbf{0}_{U-N \times 1}$. Therefore, the two constraints (11) and (12) are satisfied. The ZP extension has a simple intuitive meaning of frequency-domain interpolation. By (14), this choice is equivalent to the increase of both the frequency-domain resolution and the Doppler-domain resolution. However, the time variation of the extended channel path presents a discontinuity, which translates into an increase of the band approximation error in (16). Noteworthy, the increased approximation error does not automatically turn into a performance loss with respect to the conventional frequency-domain equalizer, at least for low Doppler spread [9].

3.3. Fourier Series (FS) Channel Approximation

A third method, proposed in [8], adopts the extended channel that minimizes the band approximation error. This method relies on the Fourier series (FS) approximation of the channel time variation, and omits the constraint $\mathbf{H}_{\mathrm{UL}} = \mathbf{H}_{\mathrm{t}}$. Specifically, let us denote with $\mathbf{h}_l$ the N-dimensional vector that contains the time variation of the l th channel path, from $n=0$ to $n=N-1$. By defining the $U \times 2Q+1$ matrix $\mathbf{F}_U^{(Q)}$ as the submatrix that contains only the first $Q+1$ and the last Q columns of $\mathbf{F}_U$, and the $M \times 2Q+1$ matrix $\mathbf{F}_U^{(M,Q)}$ as the submatrix that contains only the first M rows of $\mathbf{F}_U^{(Q)}$, with $M < U$, the FS approach constructs the extended channel matrix $\mathbf{H}_{\mathrm{et}}$ in (10) by using the U-dimensional extended channel paths $\{\mathbf{h}_l^{(\mathrm{FS})}\}_{l=0}^{L}$ obtained as the FS approximation of the N-dimensional true channel taps $\{\mathbf{h}_l\}_{l=0}^{L}$, as expressed by

$$\mathbf{h}_l^{(\mathrm{FS})} = \mathbf{F}_U^{(Q_{\mathrm{F}})} (\mathbf{F}_U^{(N,Q_{\mathrm{F}})})^{\dagger} \mathbf{h}_l, \tag{20}$$

where the superscript † denotes Moore-Penrose matrix pseudoinversion. Please observe that Q_{F} used in (20) can be different from the Q parameter used in (16) to band the extended frequency-domain channel matrix.

From (20), it is clear that by the FS approach, the first N elements of the extended channel paths do not coincide with the true channel paths. Nevertheless, as shown in the example of Fig. 1, usually the approximation is rather good. More precisely, the FS method projects the channel paths in such a way that the channel matrix in the extended frequency domain $\mathbf{H}_{\mathrm{ef}}$ in (14) is exactly banded with semi-band Q_{F}, suggesting the choice $Q = Q_{\mathrm{F}}$. Therefore, the band approximation error $\| \mathbf{H}_{\mathrm{ef}}^{(Q_{\mathrm{F}})} - \mathbf{H}_{\mathrm{ef}} \|_F$ is minimized, being virtually zero (apart from those numerical errors caused by finite-precision calculation). This exact banded structure is achieved by circularly extending the channel paths in the submatrix $\mathbf{H}_{\mathrm{UR}}$ in (10), as it happens in the OFDM case [3]. As a result of the Fourier basis periodicity, the extended channel path is periodic (with period U). From the complexity point of view, the FS channel approximation is more complex than the TC and ZP approaches, because of the linear transformation in (20).

Please note that, when the time-varying channel is estimated using a basis expansion model (BEM), the channel matrix can be estimated in the extended frequency-domain [12]. This means that, when the BEM span K is chosen equal to U, it is mathematically possible to directly estimate the diagonals of $\mathbf{H}_{\mathrm{ef}} = \mathbf{H}_{\mathrm{ef}}^{(Q_{\mathrm{F}})}$, thereby bypassing (20). However, the channel identifiability condition requires that the number of used pilot blocks is greater than or equal to the number of BEM functions used to model the time variation [12]. Hence the BEM size should be $K \ge (2Q_{\mathrm{F}}+1)N$, which is usually larger than common values used for U even for $Q_{\mathrm{F}}=1$ (in [8,12], $U=2N$). In other words, the complexity of (20) cannot be saved in practice.

3.4. Reversal Channel (RC) Extension

In order to reduce complexity while maintaining a small approximation error, we introduce a new channel extension. Our aim is to avoid the complexity increase given by (20) and to maintain the time variation continuity to keep the band approximation error at a reasonably small level. First, we note that, in the digital domain, continuity should be intended in a cyclic sense. For instance, the TC extension should not be intended as continuous, because the two edge values can be significantly different, like in the example of Fig. 1. On the other hand, the FS approximation is continuous because is periodic with period U. As a result, we propose to extend each channel path by reversing the time variation itself. This way we are able to force cyclic continuity like in the FS approach, while avoiding any calcula-

tions like in the TC and ZP approaches. Obviously, we are imposing an additional constraint, which is $U = 2N$. An example of the proposed approach, referred to as *reversal channel (RC) extension*, is shown in Fig. 1. Mathematically, the U -dimensional extended path can be expressed by

$$\mathbf{h}_l^{(\mathrm{RC})} = [\mathbf{h}_l^T \quad \tilde{\mathbf{h}}_l^T \mathbf{J}_N]^T, \tag{21}$$

where $\tilde{\mathbf{h}}_l$ is the vector that contains the time variation of the l th channel path, from $n = 1$ to $n = N$, and $\mathbf{J}_N$ is the $N \times N$ counteridentity matrix, i.e., a permutation matrix with all ones in its antidiagonal.

Intuitively, we expect that the RC approach, though less complex than the FS approach, will not maintain the zero band approximation property of the FS. Indeed, the RC extension, although continuous, does not implies the continuity of the derivatives. For instance, from Fig. 1, it is clear that for the RC the first derivative is not continuous at $n = 8$. However, differently from the FS, the channel behavior is exactly represented in the first part. As a consequence, we expect that the performance of the RC approach will not be too far from that of the FS approach. To quantify the performance of the different approaches discussed in this section, we resort to simulation results.

4. SIMULATION RESULTS

We want to compare the band approximation error and the BER performance of the equalizers described in Section 3. We assume a multipath channel with order $L = 10$, exponential power-delay profile $E\{|h[n,l]|^2\} = e^{-l/4}$, and zero-mean complex Gaussian independent random paths (Rayleigh fading). The time variation is modeled by a Jakes' Doppler spectrum with maximum Doppler spread f_D. We also assume data blocks of length $D = 118$, with i.i.d. QPSK symbols, and pilot blocks of length $P = L$, which leads to $N = 128$. At the receiver, we fix $U = 2N = 256$. For the FS method, we use $Q_\mathrm{F} = 2$.

In the first set of simulations, we assume a normalized Doppler spread $f_\mathrm{D} T_\mathrm{S} N = 0.32$. Fig. 2 illustrates the *relative squared band approximation error* (RAE), defined as

$$\mathrm{RAE}(Q) = \frac{\| \mathbf{H}_{\mathrm{ef}}^{(Q)} - \mathbf{H}_{\mathrm{ef}} \|_F^2}{\| \mathbf{H}_{\mathrm{ef}} \|_F^2} \tag{22}$$

($\mathbf{H}_\mathrm{f}^{(Q)}$ and $\mathbf{H}_\mathrm{f}$ are used for the usual frequency domain). From Fig. 2, it is evident that the RAE decreases smoothly with Q for TC, ZP, and conventional frequency-domain channel matrices, while decreases rapidly for the RC and FS extensions. Therefore, we expect that RC and FS will produce better equalization performance with respect to the other cases. Fig. 2 also confirms that the FS method produces $\mathrm{RAE}(Q) = 0$ for $Q \geq Q_\mathrm{F}$.

Fig. 3 displays the BER performance of the different equalizers, as a function of the SNR per bit, for $Q = 2$. As expected, RC and FS give the best performance. In particular, FS slightly outperforms RC. This means that FS is able to counterbalance its (non-extended) channel path approximation thanks to its reduced band approximation error. However, FS requires the extra complexity of (20). Among the other approaches, ZP yields relatively-good performance, despite its high RAE. Indeed, although the ZP extension is discontinuous at both edges, its interpolation effect produces a useful increased resolution, which is exploited by the equalizer [9].

Fig. 4 focus on the BER comparison between FS and RC for different values of Q. For $Q = 3$, the two methods gives the same performance, which coincides with that obtained by FS for $Q = 2$. This is obvious for FS, whose RAE is zero for $Q > Q_\mathrm{F} = 2$, but not for RC, whose RAE is non zero. However, RC is able to better represents the non-extended part of the channel path. This is confirmed by observing the results for $Q = 1$, where RC slightly outperforms FS, despite RC presents a higher value of RAE when $Q = 1$ (see Fig. 2).

In the second set of simulations, we assume a higher normalized Doppler spread $f_\mathrm{D} T_\mathrm{S} N = 0.64$. In this case, Fig. 5 shows for RC an alternating behavior of RAE reduction and almost-constant RAE. This is confirmed by the BER comparison of Fig. 6, where RC with $Q = 3$ produces only a minor improvement with respect to RC with $Q = 2$. This confirms the usefulness of the RAE simulations in predicting the BER behavior.

5. CONCLUSIONS

We have investigated the effect of different channel extensions on the banded structure of extended frequency-domain channel matrices that model doubly-selective channels. We proposed a new time-reversal-based channel extension that, compared with the ZP interpolation method, has the nice property to similarly increase the frequency-domain resolution without any complexity increase, while reducing the BER of banded LMMSE equalizers. Future work will focus on pilot-aided channel estimation and on receiver windows specially designed for the proposed reversal extensions.

6. REFERENCES

[1] Z. Wang and G. B. Giannakis, "Wireless multicarrier communications: where Fourier meets Shannon," *IEEE Signal Processing Mag.*, vol. 17, pp. 29-48, May 2000.

[2] H. Sari, G. Karam, and I. Jeanclaude, "Transmission techniques for digital terrestrial TV broadcasting," *IEEE Commun. Mag.*, vol. 33, pp. 100-109, Feb. 1995.

[3] W. G. Jeon, K. H. Chang, and Y. S. Cho, "An equalization technique for orthogonal frequency-division multiplexing systems in time-variant multipath channels," *IEEE Trans. Commun.*, vol. 47, pp. 27-32, Jan. 1999.

[4] P. Schniter, "Low-complexity equalization of OFDM in doubly selective channels," *IEEE Trans. Signal Processing*, vol. 52, pp. 1002-1011, Apr. 2004.

[5] L. Rugini, P. Banelli, and G. Leus, "Low-complexity banded equalizers for OFDM systems in Doppler spread channels," *EURASIP J. Appl. Signal Processing*, vol. 2006, Article ID 67404, pp. 1-13, 2006.

[6] S. Ohno, "Maximum likelihood inter-carrier interference suppression for wireless OFDM with null subcarriers," *IEEE ICASSP 2005*, Philadelphia, PA, vol. III, pp. 849-852, Mar. 2005.

[7] P. Schniter and H. Liu, "Iterative frequency-domain equalization for single-carrier systems in doubly-dispersive channels," *Asilomar Conf. on Signals, Systems, and Computers*, pp. 667-671, Nov 2004.

[8] Z. Tang and G. Leus, "Receiver design for single-carrier transmission over time-varying channels," *IEEE ICASSP 2007*, Honolulu, Hawaii, vol. 3, pp. 129-132, Apr. 2007.

[9] L. Rugini, P. Banelli, and M. Berioli, "Block equalization for single-carrier satellite communications with high-mobility receivers," *IEEE GLOBECOM 2007*, Washington, DC, Nov 2007.

[10] X. Ma, G. B. Giannakis, and S. Ohno, "Optimal training for block transmissions over doubly-selective wireless fading channels," *IEEE Trans. Signal Processing*, vol. 51, pp. 1351-1366, May 2003.

[11] J. G. Proakis, *Digital Communications*, 3rd ed. New York: McGraw-Hill, 1995.

[12] Z. Tang, *OFDM Transmission over Rapidly Changing Channels*, Ph.D Dissertation at Delft University of Technology, Netherlands, Nov. 2007.

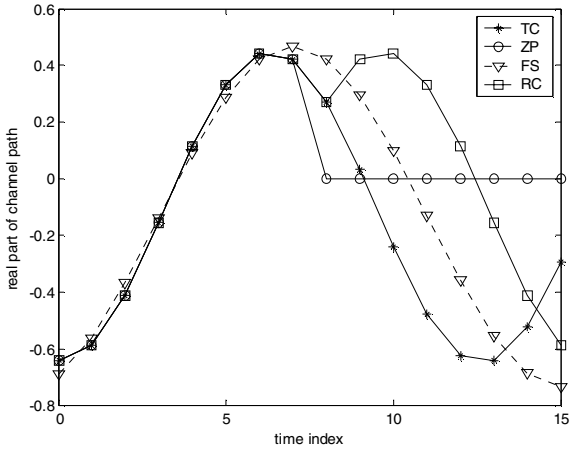

Fig. 1. Example of different channel extensions ($N = 8$, $U = 16$).

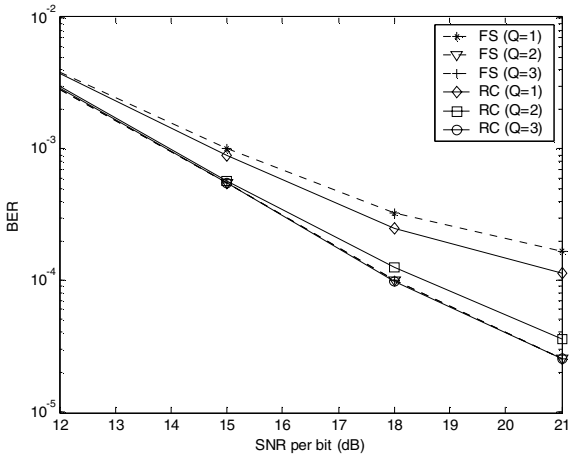

Fig. 4. BER comparison between FS and RC ($f_{\mathrm{D}}T_{\mathrm{S}}N = 0.32$).

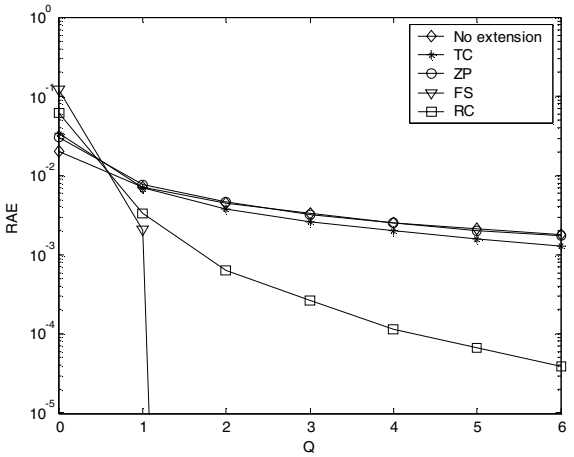

Fig. 2. Band approximation error as a function of Q ($f_{\mathrm{D}}T_{\mathrm{S}}N = 0.32$).

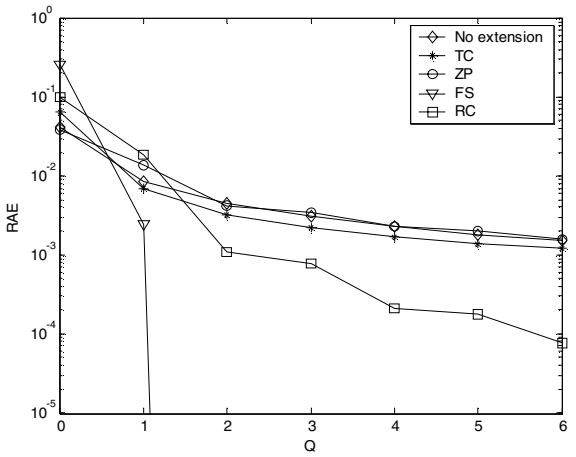

Fig. 5. Band approximation error as a function of Q ($f_{\mathrm{D}}T_{\mathrm{S}}N = 0.64$).

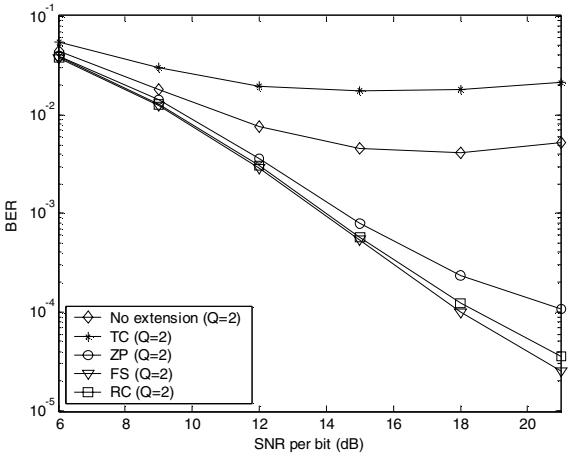

Fig. 3. BER for different channel extensions ($Q = 2$, $f_{\mathrm{D}}T_{\mathrm{S}}N = 0.32$).

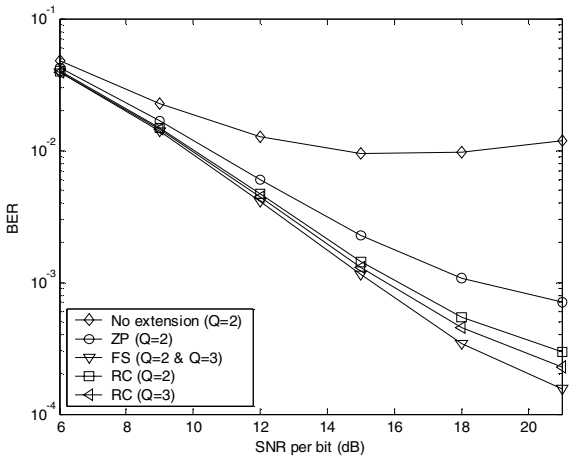

Fig. 6. BER for different channel extensions ($f_{\mathrm{D}}T_{\mathrm{S}}N = 0.64$).